

From single-layer graphene to HOPG: universal functionalization strategy with perfluoropolyether for the graphene family materials.

Eugenio Gibertini^{a,†}, Luca Gabatell^{a,b,†}, Andrea Lucotti^c, Gianlorenzo Bussetti^d, Claudia L. Bianchi^{e,f}, Luca Nobili^{a,b}, Luca Magagnin^{a,b}, Walter Navarrini^{a,b}, Maurizio Sansotera^{a,b,*}

^a Dipartimento di Chimica, Materiali e Ingegneria Chimica, Politecnico di Milano, Via Mancinelli 7, 20131 Milano, Italy

^b Consorzio Interuniversitario Nazionale per la Scienza e Tecnologia dei Materiali (UdR-PoliMi), via G. Giusti, 9, 50121 Firenze, Italy

^c Dipartimento di Chimica, Materiali e Ingegneria Chimica, Politecnico di Milano, Piazza Leonardo da Vinci 32, 20133 Milano, Italy

^d Dipartimento di Fisica, Politecnico di Milano, P.za Leonardo Da Vinci 32, 20133 Milano, Italy

^e Dipartimento di Chimica, Università degli Studi di Milano, via Golgi 19, I-20133 Milano, Italy

^f Consorzio Interuniversitario Nazionale per la Scienza e Tecnologia dei Materiali (UdR-UniMi), via G. Giusti, 9, 50121 Firenze, Italy

* Corresponding author. Tel: +39.02.2399.4770; Fax: +39.02.2399.3280; Email Address:

maurizio.sansotera@polimi.it

† Equally contributing first authors.

Codice campo modificato

Abstract

Graphene functionalization offers the opportunity to modify the chemical-physical properties of graphene, therefore broadening the variety of its possible applications. In this work, single- and few-layers graphene as well as highly oriented pyrolytic graphite (HOPG) were functionalized with perfluoropolyether (PFPE) chains via a peroxide decomposition and radical reaction. Samples were prepared using different amounts of PFPE peroxide and the effects of the treatment were studied through Raman spectroscopy, grazing angle Fourier-transform Infrared spectroscopy (GA-FTIR), X-Ray Photoelectron Spectroscopy (XPS) and water contact angle measurements. A coherent trend of F-C bonds with increasing amount of peroxidic precursor was detected, attacking the sp^2 reactive sites of the grains of graphene itself and generating new sp^3 hybridizations. The perfluorinated chains were found to give hydrophobic properties to graphenic layers, demonstrating the functionalization route as an easy and universal strategy for the preparation of hydrophobic graphenic substrates.

Highlights

- Thermal decomposition of perfluoropolyether peroxide is confirmed to be an effective method for the covalent functionalization of graphenic substrates with PFPE chains.
- Functionalization degree, as I_D/I_G ratio, is coherent with the concentration of PFPE peroxide precursor.
- Grafted PFPE chains provide hydrophobicity to the treated substrates.

Keywords: graphene, covalent functionalization, perfluoropolyethers, hydrophobicity.

1. Introduction

Graphene is a widely known and studied carbon material which shows extraordinary electrical, thermal and mechanical properties thanks to its peculiar lattice structure and electronic configuration [1,2]. It features a honeycomb lattice with a two-atoms unit cell and its band structure has been studied to show a zero-gap in correspondence with K points at the edges of its Brillouin zone [3,4]. Adding transparency in the visible range [5], the range of properties and applications of graphene becomes broadly extended over many industrial and technological fields, such as nanoelectronics [6], organic magnets [7], sensing devices [8–10], energy storage [11–15] and composites [16,17]. Other than pristine graphene properties, surface modification of graphene is able to introduce new functionalities and opens up its employment to a countless number of applications. For instance, physical and chemical properties of the standalone material can be tuned in semiconducting behaviour, magnetic properties, enhanced mechanical strength, catalytic properties and preferred interaction with species from the surrounding environment [18,19]. Graphene functionalization can be either non-covalent or covalent [20,21]. In the first case, functionalities are added to the material without altering its structure by exploiting π - π interactions with highly conjugated carbon chains. On the other hand, with covalent functionalization a strong interaction arises between graphene and the functionalizing moieties in correspondence with newly created or already present sp^3 lattice sites. The product is usually highly stable and the linkage of a vast number of chemicals is allowed, from single atoms to polymers [22–25]. Some routes for the covalent functionalization of graphene are hydrogenation [26,27], fluorination [28,29], substitution of already present oxygenated groups, nucleophilic addition and electrophilic substitution [30,31], radical reactions [32] or controlled oxidation to give graphene oxide (GO) [33]. Fluorination and perfluoroalkylation of carbon-based polyaromatic materials have already been widely studied in order to enhance their chemical-physical stability [34–36]. In particular, the fluorographene family recently attracted tremendous interest for its peculiar property and reactivity when used as precursor for the synthesis of new 2D graphene-based materials [37,38]. Functionalization of graphene with radical reactions have been already mentioned in the literature as a useful tool for graphene modification and researches using perfluorinated radicals were also reported [39,40]. Our group extensively investigated the linkage of perfluoropolyether (PFPE) to carbon-based materials, such as carbon black and MWCNTs, defining a clarified reaction mechanism and obtaining the modification of the wettability and the electronic properties of the substrates [41–45]. In particular, a radical reaction subsequent to the thermal decomposition of PFPE peroxides was found to take place and promote the formation of covalent bonds between the graphitic core of carbon-based

substrates and the PFPE segments. In this work, we investigated the perfluoroalkylation by PFPE peroxides covalent bonding on both graphenic (single- and few-layers CVD grown graphene) and graphitic (HOPG) substrates, demonstrating it as suitable approach for the surface grafting of PFPE chains to any graphene-like carbon structure. Samples were characterized by different techniques in order to provide a complete overview of the effect of the functionalization process. Raman spectroscopy, SEM, STM, AFM and optical microscopy in order to investigate their structure and GA-FTIR spectroscopy and XPS in order to study the extent of functionalization.

2. Experimental

2.1 Materials

Commercial electroformed nickel foil (GoodFellow, thickness 10 μm) was cut in piece of 1 cm \times 2 cm and used as substrates for the CVD process. Single-layer graphene (SLG) grown by CVD on Cu substrate (1.13 cm^2) was purchased by Graphenea while HOPG (grade ZYB, 20 mm \times 20 mm \times 2 mm) was obtained by SPI Supplies, Inc. PFPE was Fomblin[®] Z (Solvay Speciality Polymers), with linear structure in which the monomeric units $(\text{CF}_2\text{CF}_2\text{O})_m$, $(\text{CF}_2\text{O})_n$ and peroxidic units $(\text{O})_v$ were randomly distributed along the polymer chain: $\text{T}(\text{CF}_2\text{CF}_2\text{O})_m(\text{CF}_2\text{O})_n(\text{O})_v\text{T}'$. The chemical characteristics of the peroxidic PFPE are here reported: average molecular weight of 29000 g/mol, equivalent molecular weight of 1200 g/mol, ratio between perfluoroethylene oxide (m) and perfluoromethylene oxide (n) groups equal to 1.15, peroxidic content of 1.32%wt. and CF_3 , COF, CF_2COF as terminals (T, T'). An inert fluorinated solvent, Galden[®] HT110 (Solvay), was employed for the dissolution of PFPE peroxide.

2.2 Chemical vapour deposition of few-layer graphene on Ni

Few-layer graphene (FLG) was grown on Ni foil according to the procedure adopted in previous works [46,47]. Briefly, Ni substrates were inserted in a quartz vial and annealed in a tubular furnace under H_2 flow at 1000°C for 60 min. A pre-mixed flow of methane and hydrogen (3% CH_4) flowed for 10 min at 1000°C, then the sample was cooled to 700°C and held for other 10 min. Before starting the procedure, the vial was deoxygenated under a nitrogen flow to remove any trace of residual oxygen.

2.3 Chemical functionalization with PFPE peroxides

The functionalization of graphene and graphitic substrates with PFPE peroxide was performed readapting the protocol employed in previous studies on carbon powders [41–44]. Solutions of PFPE peroxide in Galden[®] HT110 at different concentrations, namely 0.3 g/L, 2.1 g/L and 21 g/L, were prepared by stirring for 1 h and the sample surface was then completely covered by casting the solution. The concentration of PFPE peroxide equal to 2.1 g/L was the reference value obtained by considering the formation of a monolayer of PFPE functionalizing the graphene layer, based on the stoichiometric data of PFPE peroxide reported in Paragraph 2.1. Concentrations of 0.3 g/L and 21 g/L were considered in order to observe the effect due to a functionalization with an increase and a decrease in PFPE peroxide concentration of one order of magnitude, respectively. The volume of solution required for the complete coverage of graphene as well as graphitic

substrates was evaluated experimentally and it resulted equal to 40 μL for both single and few-layers graphene and to 160 μL for HOPG, respectively. For the HOPG only, pure PFPE peroxide was also employed for comparison (HOPGP sample). Samples prepared are reported in Table 1 and labelled according to the PFPE peroxide concentration in solution. A thermal treatment in oven was then applied in N_2 atmosphere in order to promote the decomposition of the peroxide. The treatment started with 3 h at 110 $^{\circ}\text{C}$ for the evaporation of the solvent and then samples were heated to 200 $^{\circ}\text{C}$ for 2 h. Samples were then washed in Galden[®] HT110 in an ultrasonic bath at 355 W for 10 minutes, dried at 110 $^{\circ}\text{C}$ for 30 minutes under vacuum and rinsed in water 3 times. Finally, a decarboxylation thermal treatment at 200 $^{\circ}\text{C}$ for 2 h under vacuum was applied.

	Sample	PFPE (g/L)
SLG@Cu	SLG	-
	SLG0.3	0.3
	SLG2.1	2.1
	SLG21	21
FLG@Ni	FLG	-
	FLG0.3	0.3
	FLG2.1	2.1
	FLG21	21
HOPG	HOPG	-
	HOPG21	21
	HOPGP	pure

Table 1. Sample list and relative PFPE peroxide concentration. Single-layer graphene samples are labelled as SLG and few-layers graphene samples as FLG.

2.4 Chemical and physical characterization

Raman spectra were recorded with a Horiba Jobin Yvon LabRAM HR800 Raman spectrometer equipped with Olympus BX41 microscope. The excitation laser line 532 nm at 25 mW was focused by a LWD 50 \times objective on the sample surface. Spectra were recorded as a double scan integrating the signal over 30 s. Grazing angle-FTIR analysis was performed with a Thermo Nicolet 380 FT-IR Spectrometer equipped with a Smart SAGA grazing angle objective with an 80 $^{\circ}$ average angular aperture. X-ray photoelectron spectroscopy spectra were obtained using a M-probe apparatus (Surface Science Instruments). The source was monochromatic Al K_{α} radiation (1486.6 eV). A spot size of 200 $\mu\text{m} \times 750 \mu\text{m}$ and pass energy of 25 eV were used. $1s$ level hydrocarbon-contaminant carbon was taken as the internal reference at 284.6 eV. For each sample, survey analyses in the whole range of X-ray spectrum have been performed, in order to determinate the surface elemental composition. Similarly, high resolution scans around C $1s$ and O $1s$ were acquired for the determination of the chemical environment surrounding every species. A Keysight 5500 model was used for the topographic characterization. This experimental set-up allows both atomic force

(AFM) and scanning tunnelling microscopy (STM) characterization. Pristine graphite (or samples treated with very low PFPE concentration) can be studied by both AFM and STM because the sample surface is flat enough. Conversely, when HOPG undergoes a treatment with pure PFPE peroxide, STM analysis is precluded because it is not possible to reach a good stability of the STM tip. The latter was an etched W tip driven at constant current. AFM exploited Si cantilevers (NanoSensors) coated by Al to enhance the laser reflection. Images were collected in contact mode. The water contact angle instrument used was a Data Physics OCA 150, equipped with Liquavista Stingray camera and a Liquavista LED light source for background illumination. Three measures were averaged for every sample and the droplet shape was modelled with an elliptical fit through the SCA20 software (2.3.9 build 46).

3. Results and discussion

In this work we have investigated the PFPE covalent grafting route to graphenic family materials to provide a complete overview of the PFPE functionalization strategy to the whole carbon nanostructures group. PFPE chains grafting to different carbon nanostructures was already demonstrated by our group [41–45]. Both carbon black (CB) and multi-walled carbon nanotubes (MWCNTs) were covalently functionalized with PFPE chains. This functionalization route involves the homolytic cleavage by thermal decomposition of the O–O peroxidic units of PFPE chains and generation of oxygen-centered perfluorinated free radicals. In these PFPE oxyradicals, perfluoromethylene oxide ($-\text{CF}_2\text{O}$, C_1 units) or perfluoroethylene oxide units ($-\text{CF}_2\text{CF}_2\text{O}$, C_2 units) can be randomly found adjacent to the radical oxygen atoms ($\cdot\text{O}-$). The carbon-centered PFPE radicals are generated from the oxyradicals by the β -scission reactions: if the neighbouring group is a C_2 unit, a β -scission reaction occurs with the elimination of a COF_2 molecule; if the neighbour group is a C_1 unit and the successive unit is a C_2 unit, two consecutive β -scission reactions occur with elimination of two COF_2 molecules; the case of two successive C_1 units adjacent the oxyradical is quite unlikely, because C_1 units are typically less than C_2 units (C_2/C_1 ratio is 1.15, see paragraph 2.1). Perfluorinated radicals are highly reactive towards sp^2 hybridized carbon atoms and aromatic rings can act as radical scavengers. Thus, each carbon-centered PFPE radical reacts with the polycyclic moieties changing the hybridization of a single carbon atom from sp^2 to sp^3 and generating an aryl radical adduct covalently linked to a PFPE chain. During the functionalization process, these aryl radical intermediates can rearrange in several resonance structures along the bidimensional polycyclic structure of graphene until they react further by coupling with other radicals or by proton removal from defects. The overall effect of the functionalization reaction with PFPE peroxide is the covalent linkage of non-peroxidic PFPE chains the carbon-based substrate of graphene. The resulting PFPE-functionalized graphene is thermally stable on until around 400°C , that is the characteristic temperature of perfluorocarbons thermolysis [45].

3.1 Structural and chemical analyses

Raman spectroscopy is widely employed to investigate the functionalization of graphene-based materials, since Raman scattering is very sensitive to the effect of carbon hybridization transition, charge-transfer and doping induced by functionalization [48–50]. Raman spectra of pristine and functionalized SLG are reported in Figure 1a. Raman analyses for FLG21 and HOPGP (Figure S2) have not been investigated in details because of the high fluorescence induced by PFPE functionalization in these samples that prevent an accurate determination of peak position and intensity. SLG shows the typical Raman fingerprint of monolayer graphene, with G band centred at 1580 cm^{-1} , 2D at 2665 cm^{-1} and I_{2D}/I_G ratio of 2.5. As a confirmation of good quality pristine single-layer graphene, no D band is detected. According to the reaction scheme previously proposed [45], the decomposition of peroxide units results in aromatic ring opening and sp^2 to sp^3 carbon state transition. Raman spectra of functionalized SLG confirm that the reaction mechanism applies also for a pure and non-defected graphene monolayer. In fact, partial structural modification of the graphenic layer is clearly visible even at low PFPE concentration, namely sample SLG0.3, due to the appearance of the D band at 1350 cm^{-1} . As a consequence of PFPE chains grafting, both G band and 2D bands blueshift, thus shift at higher wavenumbers (Figure 1b). Shifts are shown to be as large as 21 and 34 cm^{-1} for G and 2D band respectively for SLG21 sample. Such high value of Raman bands shifts have been previously reported for strongly p-doped graphene [52,53]. Shifts in graphene Raman bands are commonly ascribed to charge-transfer and partial oxidation or reduction of the carbon lattice that results in charge-carriers concentration variation, known as doping effect [48,54]. In particular, contrarily to the G band, the 2D band blueshifts (upshifts) or redshifts (downshifts) according to respectively holes or electrons density increasing by doping. PFPE grafting reasonably induces p-doping due to the high electronegativity of CF_2 moieties along the PFPE chain, resulting in an evident blueshift of the 2D band caused by PFPE functionalization (Figure 1c). Noteworthy, the functionalization degree, as expressed by the intensity ratio between D and G bands (I_D/I_G) that reflects the sp^3 to sp^2 carbon ratio, increases with the PFPE precursor concentration, as expressed by the intensity ratio between D and G bands (I_D/I_G) that reflects the sp^3 to sp^2 carbon ratio [48,49]. Despite SLG0.3 and SLG2.1 showing similar I_D/I_G value (~ 0.4), a high disorder degree arises in case of excess PFPE concentration. The Raman spectrum of SLG21 is representative of a strongly functionalized graphene, resembling the graphene oxide one, with I_D/I_G of 0.85, demonstrating that perfluorinated radicals are efficient in graphene ring-opening reaction. This is confirmed also by the I_{2D}/I_G ratio that decreases with increasing functionalization as a result of defect induced suppression of the lattice vibration mode corresponding to the 2D peak.

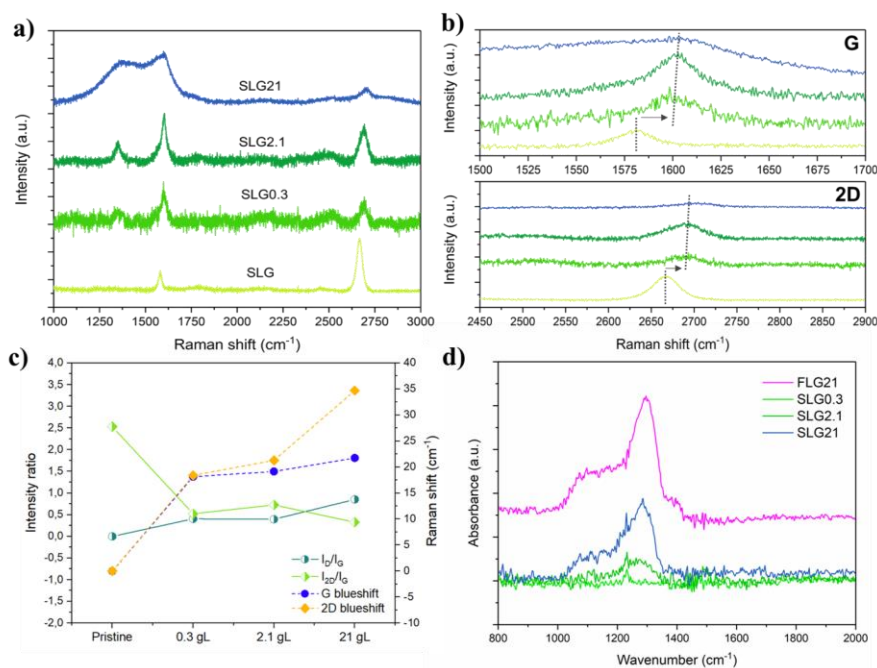


Figure 1. Raman spectra for the pristine and functionalized SLG (a). In (b) the blueshift (upshift) of both G and 2D bands is evidenced, while in (c) is reported the intensity ratio I_D/I_G and I_{2D}/I_G as well as the Raman blueshift according to the PFPE precursor concentration. (d) GA-FTIR spectra focused on the C-F spectral window for SLG samples at different PFPE peroxide concentration, compared with FLG21.

Both non-treated and treated specimens were analysed by GA-FTIR and X-Ray Photoelectron Spectroscopy in order to determine their surface chemical composition before and after the functionalization procedure. Furthermore, FTIR is able to qualitatively prove the functionalization degree according to the intensity variation of the C-F related peaks. On the other side, XPS effectively records the atomic composition of the surface, also distinguishing through the peaks, the different type of bonds. The GA-FTIR analyses performed on SLG samples after the whole functionalization procedure highlighted how the amount of bonded PFPE increases with increasing concentration of the peroxide solution (Figure 1d, the full spectra are reported in SI), coherently with Raman spectroscopy results. Absorption peaks in the 1000-1400 cm⁻¹ range can be attributed to different C-F stretching of the PFPE chains. In particular, symmetric and asymmetric CF₂ stretching at 1100 and 1290 cm⁻¹ respectively are well visible for the highly functionalized samples [55–57]. The absorption from C=C of the graphene lattice is not detected and carbon-oxygen functionalities could be ascribed to the increasing contribution in the 1000-1200 cm⁻¹ for 2.1 and 21 g/L PFPE precursor. Noteworthy, GA-FTIR spectra for SLG21 and FLG21 are almost identical, as a confirmation of PFPE

grafting occurring independently on the graphene layers number. The same results have been quantitatively confirmed by the XPS analyses. The atomic concentration of fluorine on the surface of functionalized specimens was higher the more peroxide was present in the initial solution, reaching almost 51% of fluorine in the SLG21, 57.3% for the sample FLG21 and 42.4% in the HOPG21. The difference in surface fluorine concentration is remarkable for the 21 g/L samples only, while it is strictly comparable for the SLG and FLG samples at 0.3 and 2.1 g/L. This difference could be ascribed to local inhomogeneities of the samples due to the high functionalization degree. The surface fluorine data shown in the histograms of Figure 2 are coherent with both Raman and GA-FTIR analysis, confirming that the functionalization degree is strictly dependent on the PFPE precursor concentration. Moreover, from the F/C ratio trend in SLG and FLG samples reported in Figure 2b, it is clear that a F/C ratio threshold is reached at 2.1 g/L, roughly corresponding to the C and F stoichiometry in grafted PFPE chains and revealing that the signal comes exclusively from the PFPE coating while both PFPE and graphenic substrate contribute in FLG0.3. The anomalous F/C ratio recorded on FLG21 sample can be ascribed to the layered structure of this sample, because the PFPE overlayer can attenuate the intensity of C 1s emission, thus underestimating the content of carbon atoms and overestimating this F/C ratio value.

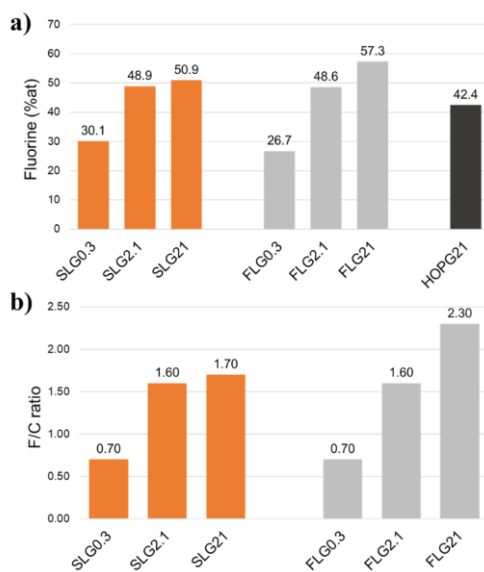


Figure 2. Fluorine atomic content of the functionalized samples (a) and F/C ratio from XPS data of SLG and FLG samples (b).

Focusing on the FLG samples functionalized with 0.3 and 21 g/L of PFPE, the high resolution XPS spectra acquired in the region of C 1s and O 1s showed the appearance of oxidized carbon atoms and oxygen atoms

not belonging to PFPE, suggesting a slight oxidation of the substrate during the functionalization procedure, probably caused by oxygen dissolved in the PFPE solution or residual oxygen in the atmosphere during the functionalization. In Figure 3 XPS spectra in the region of C 1s and O 1s for FLG0.3 and FLG21 are reported. In the case of spectra acquired in the region of C 1s, the band around 285 eV belongs to carbon atoms from graphene, both purely sp^2 at lower binding energy, and sp^3 or oxidized at higher binding energy. At around 294 eV, the band referred to carbon atoms belonging to PFPE is represented, with the two peaks at higher and lower binding energy being associated to perfluoromethyl oxide and perfluoroethyl oxide segments, respectively. The ratio between the total area associated to carbon atoms belonging to PFPE and that related to carbon atoms belonging to graphene increases with increasing amount of peroxidic precursor, due to higher coverage degree and/or growing thickness, validating the previous speculation on F/C ratio for FLG samples. Similarly, two peaks are detected in XPS spectra in the region of O 1s, one at around 532 eV belonging to oxygen atoms from oxidized graphene and one at 536 eV referred to oxygen atoms from PFPE. In XPS spectrum in the region of F 1s only one peak at 689 eV can be observed (Figure S3), ascribable to organic fluorine atoms of PFPE and confirming that there are no other fluorinated species, except for PFPE.

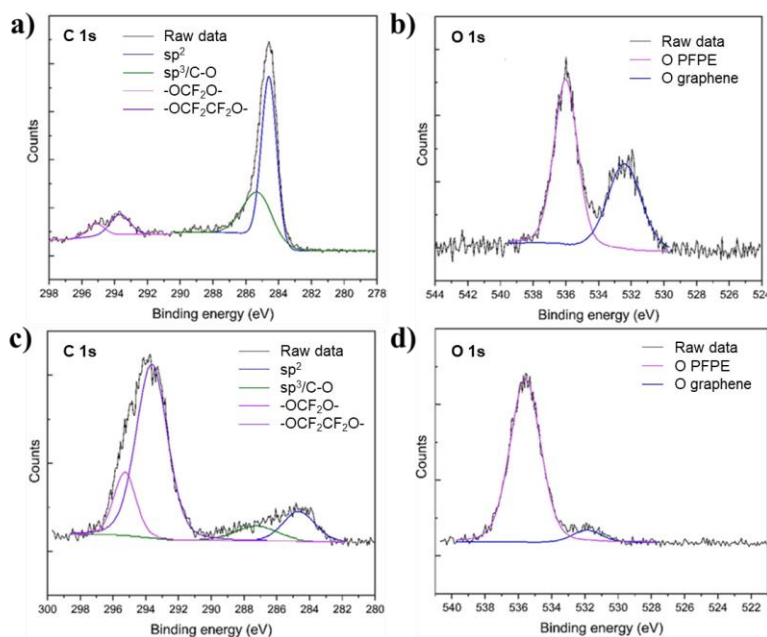


Figure 3. XPS spectra in the regions of C 1s and O 1s for FLG0.3 (a,b) and FLG21 (c,d). Peaks deconvolution was performed using the symmetrical Gaussian model without any constrain. Deconvolved peaks are assigned in legends.

3.2 AFM and STM

Figure 4a,b reports a comparison between pristine HOPG and HOPGP at the micrometre length scale, where the reader can have an idea of the morphological changes observed after functionalization. A SEM image of the treated surface is also provided in SI (Figure S3). Pristine HOPG is characterized by wide, multi atomic steps, while the functionalized sample shows a roughness enhancement and some residuals well evident from the reported image. In Figure 4b, steps are still visible but a milky overlayer, which is composed by smaller clusters and residuals, covers the graphite basal plane. In addition, some big particles are also found, randomly distributed on the graphite basal plane. However, if HOPG undergoes a milder PFPE functionalization (HOPG21), the local structure of graphite can be visualized by STM analysis, as reported in Figure 4c and 4d. This analysis can give a better idea of possible local structural changes occurring as a consequence of the functionalization.

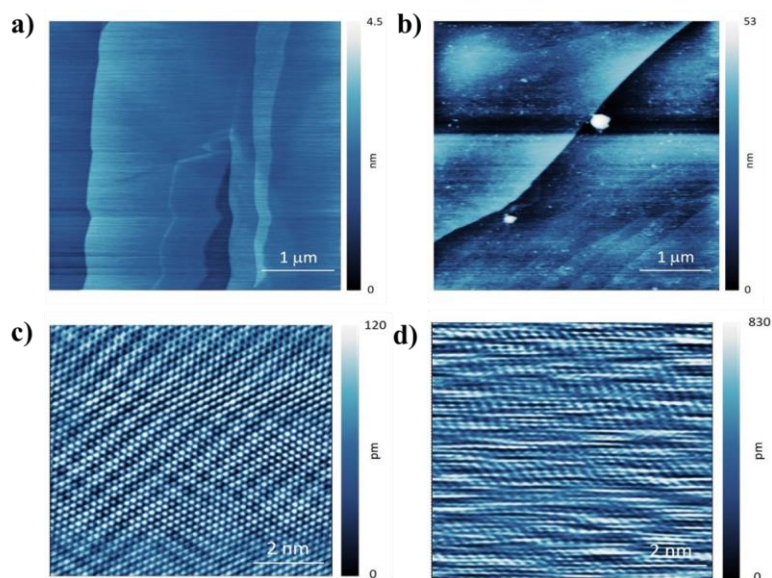


Figure 4. AFM images of pristine HOPG (a) and functionalized HOPGP with HOPGP (b), acquired in contact mode. STM images ($I_{\text{tunnel}} = 2 \text{ nA}$, $V_{\text{bias}} = 100 \text{ mV}$) of pristine (c) and HOPG21 (d).

In pristine HOPG (Figure 4c), we notice the very low roughness that can be evaluated from the colour bar. By PFPE grafting, the roughness increases of about a factor of 7 but, more interestingly, the atomic resolution is perturbed by tip slipping along the scanning direction. It is worth noting that the slipping covers some lattice parameters along the scanning direction while, in the orthogonal one, they are confined within the atomic size. The tip slipping is consequence of the surface chemical treatment. We speculate that the high spatial confinement of such perturbations can be an indirect consequence of the PFPE peroxide reaction

being localized on the graphite carbon atoms of the basal plane. Despite the difficulties in obtaining a stable STM image preclude an analysis of the sample wettability, they suggest that the STM tip can move, bend, or distort the PFPE molecule. This strong sample-tip interaction precludes a clear visualization of the surface sample apart the HOPG atomic structure at the background.

3.3 Wettability

Water static contact angle measurements were performed on all PFPE-functionalized samples and are shown in Figure 5. Fluorinated polymers are well known to be highly hydrophobic due to the intrinsic low surface-tension of fluorinated surfaces. Both SLG and FLG samples showed a coherent trend with an increasing contact angle with increasing concentration of peroxide solution, in agreement with XPS data that report a growing surface fluorine content related to PFPE chains. For the SLG samples, the water contact angle (CA) is raised from 90° of the pristine substrate to around 100° for the SLG0.3 and 108° for SLG2.1. At higher functionalization degree, no evident raising in CA is observed. Despite the higher surface fluorine content, the introduction of hydrophilic oxygen functionalities, detected by XPS, can effectively mitigate the hydrophobic effect of CF₂ moieties resulting in almost constant CA value. On the other hand, F/C ratio for SLG samples revealed that at PFPE concentration of 2.1 g/L a PFPE covering layer was already produced. The same trend was found for the FLG, where the threshold CA is achieved even at low PFPE concentration and only a slight but monotonous CA increasing is recorded. At last, HOPG sample reached the highest possible water static contact angle of 116°, approaching the value of 115° typical of fully fluorinated flat surfaces.

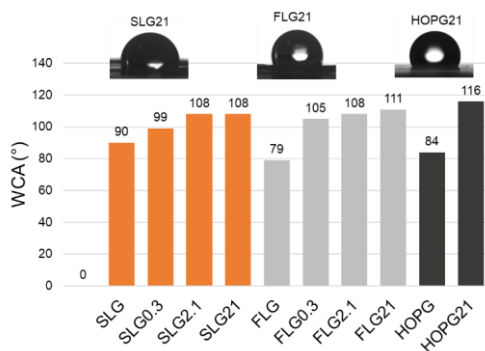


Figure 5. Water static contact angle (CA) values for pristine and functionalized samples with solutions of PFPE peroxide at different concentrations.

4. Conclusions

Different graphenic substrates, from single-layer graphene to HOPG, were successfully functionalized with perfluoropolyether chains. PFPE peroxide thermal decomposition was able to initiate the radical attack to sp²

carbon, promoting ring opening and covalent grafting of the PFPE chains. A coherent trend of the functionalization degree and fluorine atomic amount, detected on the surfaces of the samples, perfectly matched the trend of the PFPE concentration. Hydrophobic properties were achieved and confirmed by the water static contact angles recorded after the functionalization of the substrates. In summary, it is demonstrated that PFPE can be successfully grafted to any carbon material, regardless of the defectivity of the substrates as demonstrated by the high fluorine atomic content detected on HOPG surface. As a consequence, adding these results to previous works, our method is proposed as a universal strategy for PFPE covalent functionalization applicable to carbonaceous materials.

Bibliography

- [1] L.P. Biró, P. Nemes-Incze, P. Lambin, Graphene: nanoscale processing and recent applications, *Nanoscale*. 4 (2012) 1824–1839. <https://doi.org/10.1039/C1NR11067E>.
- [2] X. Huang, Z. Yin, S. Wu, X. Qi, Q. He, Q. Zhang, Q. Yan, F. Boey, H. Zhang, Graphene-Based Materials: Synthesis, Characterization, Properties, and Applications, *Small*. 7 (2011) 1876–1902. <https://doi.org/10.1002/sml.201002009>.
- [3] M. Allen, V. Tung, R. Kaner, Honeycomb carbon: A review of graphene, *Chemical Reviews*. 110 (2010) 132–145. <https://doi.org/10.1021/cr900070d>.
- [4] L.M. Malard, M.A. Pimenta, G. Dresselhaus, M.S. Dresselhaus, Raman spectroscopy in graphene, *Physics Reports*. 473 (2009) 51–87. <https://doi.org/10.1016/j.physrep.2009.02.003>.
- [5] J.K. Wassei, R.B. Kaner, Graphene, a promising transparent conductor, *Materials Today*. 13 (2010) 52–59. [https://doi.org/10.1016/S1369-7021\(10\)70034-1](https://doi.org/10.1016/S1369-7021(10)70034-1).
- [6] K.I. Bolotin, K.J. Sikes, Z. Jiang, M. Klima, G. Fudenberg, J. Hone, P. Kim, H.L. Stormer, Ultrahigh electron mobility in suspended graphene, *Solid State Communications*. 146 (2008) 351–355. <https://doi.org/10.1016/j.ssc.2008.02.024>.
- [7] J. Tuček, K. Holá, A.B. Bourlinos, P. Błoński, A. Bakandritsos, J. Ugoletti, M. Dubecký, F. Karlický, V. Ranc, K. Čépe, M. Otyepka, R. Zbořil, Room temperature organic magnets derived from sp³ functionalized graphene, *Nat Commun*. 8 (2017) 14525. <https://doi.org/10.1038/ncomms14525>.
- [8] A. Nag, A. Mitra, S.C. Mukhopadhyay, Graphene and its sensor-based applications: A review, *Sensors and Actuators A: Physical*. 270 (2018) 177–194. <https://doi.org/10.1016/j.sna.2017.12.028>.
- [9] S.-H. Bae, Y. Lee, B.K. Sharma, H.-J. Lee, J.-H. Kim, J.-H. Ahn, Graphene-based transparent strain sensor, *Carbon*. 51 (2013) 236–242. <https://doi.org/10.1016/j.carbon.2012.08.048>.
- [10] H.J. Yoon, D.H. Jun, J.H. Yang, Z. Zhou, S.S. Yang, M.M.-C. Cheng, Carbon dioxide gas sensor using a graphene sheet, *Sensors and Actuators B: Chemical*. 157 (2011) 310–313. <https://doi.org/10.1016/j.snb.2011.03.035>.
- [11] Y. Wang, Z. Shi, Y. Huang, Y. Ma, C. Wang, M. Chen, Y. Chen, Supercapacitor Devices Based on Graphene Materials, *J. Phys. Chem. C*. 113 (2009) 13103–13107. <https://doi.org/10.1021/jp902214f>.
- [12] L.L. Zhang, R. Zhou, X.S. Zhao, Graphene-based materials as supercapacitor electrodes, *J. Mater. Chem.* 20 (2010) 5983–5992. <https://doi.org/10.1039/C000417K>.
- [13] E. Yoo, J. Kim, E. Hosono, H. Zhou, T. Kudo, I. Honma, Large Reversible Li Storage of Graphene Nanosheet Families for Use in Rechargeable Lithium Ion Batteries, *Nano Lett.* 8 (2008) 2277–2282. <https://doi.org/10.1021/nl800957b>.
- [14] A. Bakandritsos, D.D. Chronopoulos, P. Jakubec, M. Pykal, K. Čépe, T. Steriotis, S. Kalytchuk, M. Petr, R. Zbořil, M. Otyepka, High-Performance Supercapacitors Based on a Zwitterionic Network of Covalently Functionalized Graphene with Iron Tetraaminophthalocyanine, *Advanced Functional Materials*. 28 (2018) 1801111. <https://doi.org/10.1002/adfm.201801111>.
- [15] I. Tantis, A. Bakandritsos, D. Zaoralová, M. Medved', P. Jakubec, J. Havláková, R. Zbořil, M. Otyepka, Covalently Interlinked Graphene Sheets with Sulfur-Chains Enable Superior Lithium–Sulfur Battery

- Cathodes at Full-Mass Level, *Advanced Functional Materials*. 31 (2021) 2101326. <https://doi.org/10.1002/adfm.202101326>.
- [16] S. Stankovich, D.A. Dikin, G.H.B. Dommett, K.M. Kohlhaas, E.J. Zimney, E.A. Stach, R.D. Piner, S.T. Nguyen, R.S. Ruoff, Graphene-based composite materials, *Nature*. 442 (2006) 282–286. <https://doi.org/10.1038/nature04969>.
- [17] X. Wei, D. Li, W. Jiang, Z. Gu, X. Wang, Z. Zhang, Z. Sun, 3D Printable Graphene Composite, *Scientific Reports*. 5 (2015) 11181. <https://doi.org/10.1038/srep11181>.
- [18] T. Kuila, S. Bose, A.K. Mishra, P. Khanra, N.H. Kim, J.H. Lee, Chemical functionalization of graphene and its applications, *Progress in Materials Science*. 57 (2012) 1061–1105. <https://doi.org/10.1016/j.pmatsci.2012.03.002>.
- [19] D.W. Boukhvalov, M.I. Katsnelson, Chemical functionalization of graphene, *Journal of Physics Condensed Matter*. 21 (2009) 1–12. <https://doi.org/10.1088/0953-8984/21/34/344205>.
- [20] V. Georgakilas, M. Otyepka, A.B. Bourlinos, V. Chandra, N. Kim, K.C. Kemp, P. Hobza, R. Zboril, K.S. Kim, Functionalization of graphene: Covalent and non-covalent approaches, derivatives and applications, *Chemical Reviews*. 112 (2012) 6156–6214. <https://doi.org/10.1021/cr3000412>.
- [21] V. Georgakilas, J.N. Tiwari, K.C. Kemp, J.A. Permana, A.B. Bourlinos, K.S. Kim, R. Zboril, Noncovalent Functionalization of Graphene and Graphene Oxide for Energy Materials, Biosensing, Catalytic, and Biomedical Applications, *Chem. Rev.* 116 (2016) 5464–5519. <https://doi.org/10.1021/acs.chemrev.5b00620>.
- [22] Y. Liu, L. Jiang, H. Wang, H. Wang, W. Jiao, G. Chen, P. Zhang, D. Hui, X. Jian, A brief review for fluorinated carbon: synthesis, properties and applications, *Nanotechnology Reviews*. 8 (2019) 573–586. <https://doi.org/10.1515/ntrev-2019-0051>.
- [23] M. Barrejón, A. Primo, M.J. Gómez-Escalonilla, J.L.G. Fierro, H. García, F. Langa, Covalent functionalization of N-doped graphene by N-alkylation, *Chem. Commun.* 51 (2015) 16916–16919. <https://doi.org/10.1039/C5CC06285C>.
- [24] M. Fang, K. Wang, H. Lu, S. Nutt, Covalent polymer functionalization of graphene nanosheets and mechanical properties of composites, *Journal of Materials Chemistry*. 19 (2009) 7098–7105. <https://doi.org/10.1039/b908220d>.
- [25] M. Fang, K. Wang, H. Lu, S. Nutt, Single-layer graphene nanosheets with controlled grafting of polymer chains, *Journal of Materials Chemistry*. 20 (2010) 1982–1992. <https://doi.org/10.1039/b919078c>.
- [26] D.W. Boukhvalov, M.I. Katsnelson, A.I. Lichtenstein, Hydrogen on graphene : Electronic structure, total energy, structural distortions and magnetism from first-principles calculations, *Physical Review B*. 77 (2008) 1–7. <https://doi.org/10.1103/PhysRevB.77.035427>.
- [27] K.E. Whitener, Review Article: Hydrogenated graphene: A user's guide, *Journal of Vacuum Science & Technology A*. 36 (2018) 05G401. <https://doi.org/10.1116/1.5034433>.
- [28] J.T. Robinson, J.S. Burgess, C.E. Junkermeier, S.C. Badescu, T.L. Reinecke, F.K. Perkins, M.K. Zalalutdniov, J.W. Baldwin, J.C. Culbertson, P.E. Sheehan, E.S. Snow, Properties of fluorinated graphene films, *Nano Letters*. 10 (2010) 3001–3005. <https://doi.org/10.1021/nl101437p>.
- [29] W. Feng, P. Long, Y. Feng, Y. Li, Two-Dimensional Fluorinated Graphene: Synthesis, Structures, Properties and Applications, *Advanced Science*. 3 (2016) 1500413. <https://doi.org/10.1002/advs.201500413>.
- [30] X. Xu, P. Li, L. Zhang, X. Liu, H.-L. Zhang, Q. Shi, B. He, W. Zhang, Z. Qu, P. Liu, Covalent Functionalization of Graphene by Nucleophilic Addition Reaction: Synthesis and Optical-Limiting Properties, *Chemistry – An Asian Journal*. 12 (2017) 2583–2590. <https://doi.org/10.1002/asia.201700899>.
- [31] S. Lai, Y. Jin, X. Sun, J. Pan, W. Du, L. Shi, Aqueous-based bromination of graphene by electrophilic substitution reaction: a defect-free approach for graphene functionalization, *Res Chem Intermed*. 44 (2018) 3523–3536. <https://doi.org/10.1007/s11164-018-3322-3>.
- [32] Y. Li, Z. Jian, M. Lang, C. Zhang, X. Huang, Covalently Functionalized Graphene by Radical Polymers for Graphene-Based High-Performance Cathode Materials, *ACS Appl. Mater. Interfaces*. 8 (2016) 17352–17359. <https://doi.org/10.1021/acsami.6b05271>.

- [33] D.C. Marcano, D.V. Kosynkin, J.M. Berlin, A. Sinitskii, Z. Sun, A. Slesarev, L.B. Alemany, W. Lu, J.M. Tour, Improved Synthesis of Graphene Oxide, *ACS Nano*. 4 (2010) 4806–4814. <https://doi.org/10.1021/nn1006368>.
- [34] K.C. Rippy, N.J. DeWeerd, I. V. Kuvychko, Y.S. Chen, S.H. Strauss, O. V. Boltalina, Fluorination-Induced Evolution of Columnar Packing in Fluorous Triphenylenes and Benzotriphenylenes, *ChemPlusChem*. 83 (2018) 1066. <https://doi.org/10.1002/cplu.201800572>.
- [35] V. Nellissery Viswanathan, A.J. Ferguson, J.R. Pfeilsticker, B.W. Larson, L.E. Garner, C.P. Brook, S.H. Strauss, O. V. Boltalina, P.C. Ramamurthy, W.A. Braunecker, Strategic fluorination of polymers and fullerenes improves photostability of organic photovoltaic blends, *Organic Electronics: Physics, Materials, Applications*. 62 (2018) 685–694. <https://doi.org/10.1016/j.orgel.2018.08.045>.
- [36] H. Fujimoto, A. Tressaud, Long-term stability of fluorine-graphite intercalation compound prepared under high pressure of fluorine, *Carbon*. 82 (2015) 176–183. <https://doi.org/10.1016/j.carbon.2014.10.060>.
- [37] D.D. Chronopoulos, A. Bakandritsos, M. Pykal, R. Zbořil, M. Otyepka, Chemistry, properties, and applications of fluorographene, *Applied Materials Today*. 9 (2017) 60–70. <https://doi.org/10.1016/j.apmt.2017.05.004>.
- [38] M. Medved', G. Zoppellaro, J. Ugolotti, D. Matochová, P. Lazar, T. Pospíšil, A. Bakandritsos, J. Tuček, R. Zbořil, M. Otyepka, Reactivity of fluorographene is triggered by point defects: beyond the perfect 2D world, *Nanoscale*. 10 (2018) 4696–4707. <https://doi.org/10.1039/C7NR09426D>.
- [39] L.-H. Liu, M.M. Lerner, M. Yan, Derivatization of Pristine Graphene with Well-Defined Chemical Functionalities, *Nano Lett.* 10 (2010) 3754–3756. <https://doi.org/10.1021/nl1024744>.
- [40] L.-H. Liu, M. Yan, Functionalization of pristine graphene with perfluorophenyl azides, *J. Mater. Chem.* 21 (2011) 3273–3276. <https://doi.org/10.1039/C0JM02765K>.
- [41] M. Sansotera, W. Navarrini, M. Gola, G. Dotelli, P.G. Stampino, C.L. Bianchi, Conductivity and superhydrophobic effect on PFPE-modified porous carbonaceous materials, *International Journal of Hydrogen Energy*. 37 (2012) 6277–6284. <https://doi.org/10.1016/j.ijhydene.2011.07.041>.
- [42] M. Sansotera, C.L. Bianchi, G. Lecardi, G. Marchionni, P. Metrangolo, G. Resnati, W. Navarrini, Highly Hydrophobic Carbon Black Obtained by Covalent Linkage of Perfluorocarbon and Perfluoropolyether Chains on the Carbon Surface, *Chem. Mater.* 21 (2009) 4498–4504. <https://doi.org/10.1021/cm901271q>.
- [43] M. Sansotera, W. Navarrini, M. Gola, C.L. Bianchi, P. Wormald, A. Famulari, M. Avataneo, Peroxidic perfluoropolyether for the covalent binding of perfluoropolyether chains on carbon black surface, *Journal of Fluorine Chemistry*. 132 (2011) 1254–1261. <https://doi.org/10.1016/j.jfluchem.2011.07.018>.
- [44] S. Talaemashhadi, M. Sansotera, C. Gambarotti, A. Famulari, C.L. Bianchi, P. Antonio Guarda, W. Navarrini, Functionalization of multi-walled carbon nanotubes with perfluoropolyether peroxide to produce superhydrophobic properties, *Carbon*. 59 (2013) 150–159. <https://doi.org/10.1016/j.carbon.2013.03.003>.
- [45] M. Sansotera, W. Navarrini, G. Resnati, P. Metrangolo, A. Famulari, C.L. Bianchi, P.A. Guarda, Preparation and characterization of superhydrophobic conductive fluorinated carbon blacks, *Carbon*. 48 (2010) 4382–4390. <https://doi.org/10.1016/j.carbon.2010.07.052>.
- [46] L. Pedrazzetti, L. Nobili, L. Magagnin, R. Bernasconi, A. Lucotti, P. Soltani, A. Mezzi, S. Kaciulis, Growth and characterization of ultrathin carbon films on electrodeposited Cu and Ni, *Surface and Interface Analysis*. 49 (2017) 1088–1094. <https://doi.org/10.1002/sia.6281>.
- [47] L. Nobili, L. Magagnin, R. Bernasconi, F. Livolsi, L. Pedrazzetti, A. Lucotti, S.K. Balijepalli, A. Mezzi, S. Kaciulis, R. Montanari, Investigation of graphene layers on electrodeposited polycrystalline metals, *Surface and Interface Analysis*. 48 (2016) 456–460. <https://doi.org/10.1002/sia.5996>.
- [48] A.C. Ferrari, Raman spectroscopy of graphene and graphite: Disorder, electron–phonon coupling, doping and nonadiabatic effects, *Solid State Communications*. 143 (2007) 47–57. <https://doi.org/10.1016/j.ssc.2007.03.052>.
- [49] A.C. Ferrari, J.C. Meyer, V. Scardaci, C. Casiraghi, M. Lazzeri, F. Mauri, S. Piscanec, D. Jiang, K.S. Novoselov, S. Roth, A.K. Geim, Raman Spectrum of Graphene and Graphene Layers, *Phys. Rev. Lett.* 97 (2006) 187401. <https://doi.org/10.1103/PhysRevLett.97.187401>.

- [50] L.M. Malard, M.A. Pimenta, G. Dresselhaus, M.S. Dresselhaus, Raman spectroscopy in graphene, *Physics Reports*. 473 (2009) 51–87. <https://doi.org/10.1016/j.physrep.2009.02.003>.
- [51] Y.Y. Wang, Z.H. Ni, Z.X. Shen, H.M. Wang, Y.H. Wu, Interference enhancement of Raman signal of graphene, *Appl. Phys. Lett.* 92 (2008) 043121. <https://doi.org/10.1063/1.2838745>.
- [52] G. Ahn, S. Ryu, Reversible sulfuric acid doping of graphene probed by in-situ multi-wavelength Raman spectroscopy, *Carbon*. 138 (2018) 257–263. <https://doi.org/10.1016/j.carbon.2018.05.065>.
- [53] M.W. Iqbal, A.K. Singh, M.Z. Iqbal, J. Eom, Raman fingerprint of doping due to metal adsorbates on graphene, *J. Phys.: Condens. Matter*. 24 (2012) 335301. <https://doi.org/10.1088/0953-8984/24/33/335301>.
- [54] B. Tang, H. Guoxin, H. Gao, Raman Spectroscopic Characterization of Graphene, *Applied Spectroscopy Reviews*. 45 (2010) 369–407. <https://doi.org/10.1080/05704928.2010.483886>.
- [55] J. Piowarczyk, R. Jędrzejewski, D. Moszyński, K. Kwiatkowski, A. Niemczyk, J. Baranowska, XPS and FTIR Studies of Polytetrafluoroethylene Thin Films Obtained by Physical Methods, *Polymers*. 11 (2019) 1629. <https://doi.org/10.3390/polym11101629>.
- [56] Y. Gao, Y. Huang, S. Feng, G. Gu, F.-L. Qing, Novel superhydrophobic and highly oleophobic PFPE-modified silica nanocomposite, *J Mater Sci*. 45 (2010) 460–466. <https://doi.org/10.1007/s10853-009-3962-1>.
- [57] J. Sun, A. Li, F. Su, Excellent Lubricating Ability of Functionalization Graphene Dispersed in Perfluoropolyether for Titanium Alloy, *ACS Appl. Nano Mater.* 2 (2019) 1391–1401. <https://doi.org/10.1021/acsanm.8b02282>.